Dynamics, Spectra, and Temperatures of Silicon Combustion in the pSi–O_2 System

Y.A. Baranyshyn, K.N. Kasparov, P.N. Krivosheyev, V.N. Mironov, O.G. Penyazkov, and L.Yu. Roshchin
A.V. Luikov Heat and Mass Transfer Institute, National Academy of Sciences of Belarus,
15 P. Brovka Str., Minsk, 220072, Belarus

The ability of porous silicon (pSi) to maintain oxidation reactions that lead to combustion and explosion [1, 2] allows treating it as a component of high-energy fuels. In work [3] an explosive system is described, where at cryogenic temperatures (4.2–90 K) the interacting atoms are in contact on an atomic scale: hydrogenated porous silicon whose pores are filled by liquid or condensed oxygen. By virtue of this, it is of interest to study the interaction of pSi with molecular oxygen – the most wide-spread oxidizer in nature.

A pSi layer was formed on 100-mm-diameter and 0.45-mm-thick wafers of single-crystal silicon with hollow conductance. The wafers had specific resistance OF 12 $\Omega \cdot cm^2$ (KDB-12) and crystallographic orientation {100} and were covered by an aluminum layer on their backside. The pSi layer formation occurred in AN electrolyte based on hydrofluoric acid (HF), with a system of nanosized channels oriented mainly deep into the wafer being formed in the single crystal and having a maximum size distribution of pores in the range of 5–10 nm. The mean characteristics of the pSi samples studied in eight regimes of their formation (further on the text - Conditions) are listed in Table 1.

Table 1: Characteristics of porous layers in different regimes of anodizing

Conditions	1	2	3	4	5	6	7	8
Layer thickness *h*, μm	19	39	34	68	47	104	61	135*
Layer porosity *p*, %	64	55	61	54	66	52	70	50

* – linear extrapolation

The experiments on pSi combustion were conducted in a steel test chamber with a wall thickness from 10 to 15 mm that can resist an excess pressure of up to 35 bar (Fig. 1). The inner volume of the chamber was about 2 L (400 × 100 × 50 mm). One wall was equipped with a double-layer window made of 30-mm-thick K8 optical glass and 9.5-mm-thick transparent polycarbonate (protecting layer) with an aperture of 128 × 102 mm. The pressure in the chamber during oxygen supply was controlled by a manometer.

Correspondence to: mirvit33@gmail.com

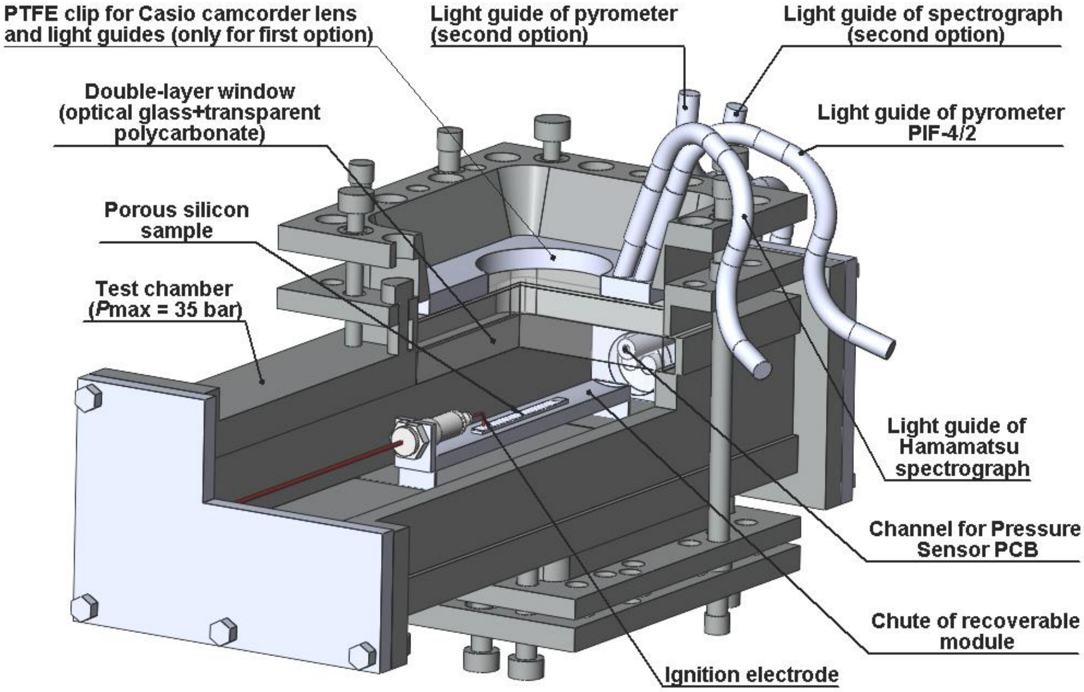

Figure 1. The blocks and elements of the experimental setup for research of pSi combustion in high pressure oxygen

Samples of pSi with a length of up to 70 mm and widths 2.3, 5, and 10 mm were used in the experiments. Scanning-electron microscopy and X-ray microanalysis were performed for identify pSi structure of each sample.

The sample was placed in the chute of recoverable module with its porous layer upward. The minimum distance from the sample to the window surface was 35 mm with a horizontal window (Fig. 1), when the processes of pSi combustion were recorded by Casio EX-F1 (300 fps) digital video camera. In the case of recording the combustion processes with camera Fastcam SA-X2 [12,500 fps (1024 × 1024 pixel); 480,000 fps max], with a vertical orientation of the window (second option), the distance from the sample to the side walls (glass and steel) was at a sample width of 5 mm at least 22 mm. For combustion initiation, a high-voltage electrode that provided a breakdown between the electrode and the pSi surface in air at a gap size of 8–10 mm ($U_{\text{break}} > 16$ kV) was mounted above the sample. The gap size decreased as the oxygen pressure increased.

The combustion temperatures were measured by the method of photoemission analysis of radiation with the aid of a photoemission pyrometer. The time resolution of the pyrometer is 5 μs, with the measurement error of 10–15%. The radiation spectrum in the course of combustion (up to 6 successive data sets with duration of 19 ms) was recorded through an optical light guide by a Hamamatsu C10029 spectrograph. For optical diagnostics the radiation was emitted through a window with an aperture of 128 × 102 mm or through a window with thickness 8 mm and aperture 30 mm in the end flange of the test chamber, when camera Fastcam SA-X2 was used (second option). The pressure in the chamber was measured by a PCB 103B12 Piezotronics pressure sensor.

Four regimes of pSi combustion in oxygen have been established. Close to the limiting pressures the combustion rate increases weakly with the value of h, the combustion zones extend mainly along the edges of samples (Fig. 2a), with subsequent initiation of transverse reaction fronts propagating with velocities 2–3 times lower than those along the edges. It should be noted that, for the first time, the V-shaped front of combustion of porous silicon was apparently described in [4]. In our case, however, the oxidizer is molecular oxygen, not solid (sodium perchlorate).

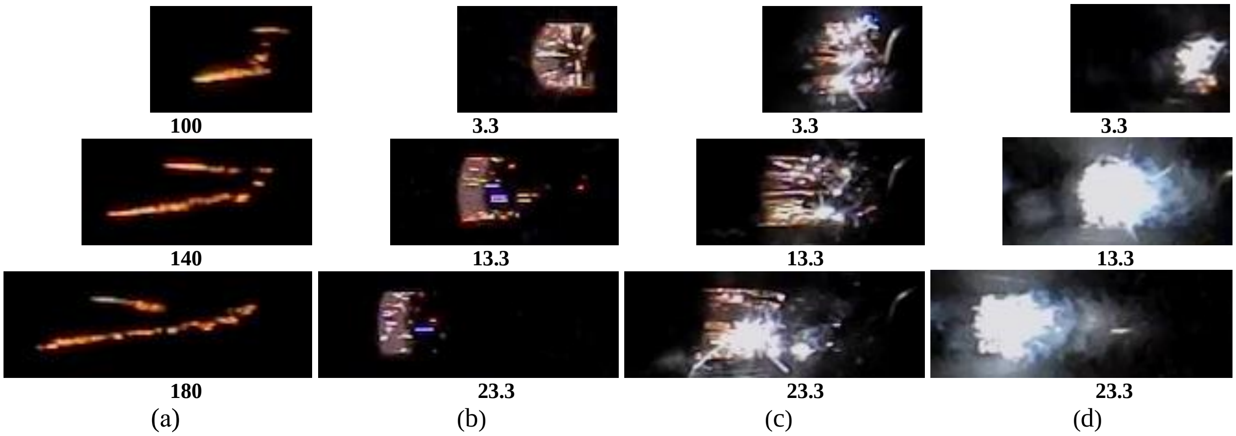

Figure 2. Regimes of pSi combustion: (a) ***smoulder*** (sample of Conditions 4, P = 5 bar); (b) ***frontal*** (sample of Conditions 1, P = 25 bar); (c) ***hybrid*** (sample of Conditions 2, P = 15 bar; (d) ***aerosol*** (sample of Conditions 1, P = 27.5 bar). Scales of images are the same, bold figures under the frames indicate time from the instant of ignition, ms.

As the pressure increases, the combustion moves from the initiation point along the radius, thus forming a diverging circular front, which, on reaching the sample edges, propagates across the sample at a constant velocity (Fig. 2b). Similar behavior of the combustion front of the pSi–$NaClO_4$ system is also described in [4], however, the pSi–O_2 system is characterized by the presence of a chemical reaction zone of constant-length (including in the initial radial-combustion region), which comparable in size to the sample width.

As the porous layer thickness or initial pressure increase, the ejection of the porous layer particles occurs behind the combustion front. The ejected particles form an aerosol above the surface of the sample that burns down intensely (Fig. 2c). As the initial pressure increases again, the aerosol combustion moves closer to the front and, finally, virtually merges with it (Fig. 2d).

The velocity of combustion propagation V throughout the porous layer changes from 0.15 to 7.6 m/s and, as a rule, increases with oxygen pressure and layer thickness. So, $V_{\max}$ = 1.1 m/s at h = 19 μm and 7.6 m/s at h = 61 μm. At the same time, the mass velocity of aerosol combustion, estimated by the intensity of radiation from the reaction zone, increases several orders of magnitude with the indicated increase of h. The pressure dependence of the mass velocity of disperse system combustion is similar (e.g., the increase is 2-3 orders of magnitude with pressure increase from 20 to 30 bar).

An analysis of combustion fronts propagation throughout the samples $S_i(t)$ shows that in most cases the process occurs virtually at a constant velocity and only at pressures close to P_{ignit} the initial portions of the curves in some cases have a smaller slope, which is caused by the low heat release at initiation. The slope of the $S_i(t)$ curves monotonically increases with pressure.

The combustion velocity depends not only on the thickness of the layer but also on its porosity. So, for Conditions 5 (h = 47 μm) the value of V, starting from medium pressures, is usually much higher than for Conditions 4 (h = 68 μm), and for Conditions 7 (h = 61 μm) it is practically always higher than for Conditions 6 (h = 104 μm). Here, the porosity for Conditions 5 is by 22% higher and for Conditions 7 by 35% than in the cases compared. This is because high porosity provides better fuel-to-oxidizer ratio and simplifies oxygen transport into the combustion zone.

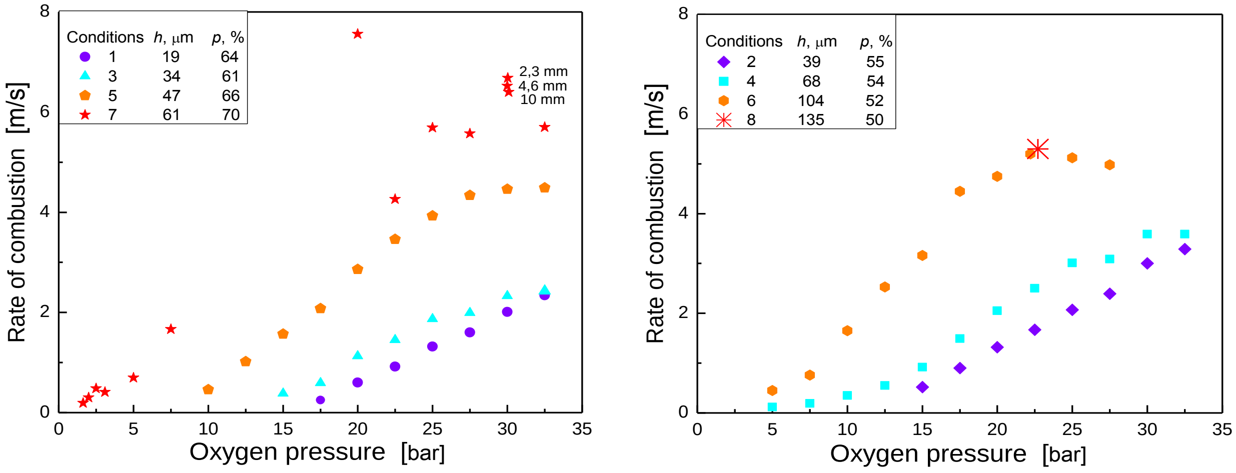

(a) (b)

Figure 2. Velocity of pSi combustion as a function of oxygen pressure for samples of Conditions: (a) 1, 3, 5, 7; (b) 2, 4, 6, 8. Mean values of the porous layer thickness *h* and porosity *p* are indicated.

Fig. 3 shows the values of the stoichiometry coefficients calculated on the basis of the skeleton mass and the oxidant mass in the pores. The results are presented for samples of the Conditions under which deviations from directly proportional dependences of the combustion velocities on oxygen pressure begin. It is seen that for Conditions with a shorter wafers formation time (15 minutes), when the porosity is higher, the amount of oxidizer is insufficient, but not to same extent as in modes with an anodizing time of 30 minutes.

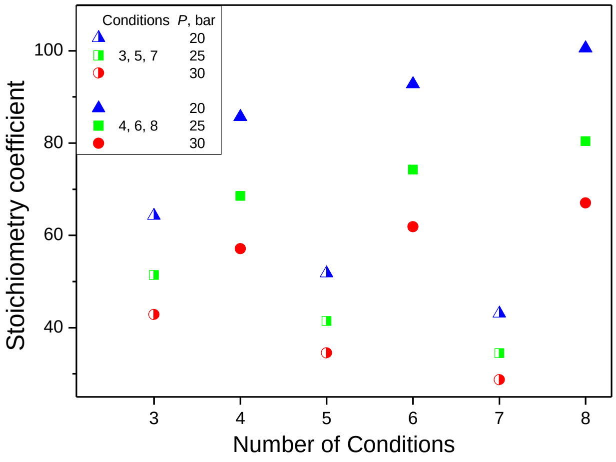

Figure 3. The values of the coefficients of stoichiometry for the $pSi-O_2$ system

Note that in the considered range of porosity about 20% of the Si atoms are located at the surface of the nanocrystals [5] and only the surface silicon atoms are supposed to be converted into SiO_2 [3].Thus, for frontal combustion, it is possible to assume that the actual values of the coefficients of stoichiometry are five times lower than those shown in Fig. 3. But even in this case, the lack of oxygen in the porous layer is very significant.

If we use the combustion model of the porous layer proposed in [3], the portion of oxygen that can participate in the oxidation of pSi decreases even more, since in step B part of it goes to oxidize the hydrogen removed from the surface of the hydrogenated porous silicon.

In our opinion, this proves that the observed degree of oxidation in the process of frontal combustion is impossible without attracting the oxygen of gas phase to the process, and the low combustion velocity is due to the complexity of transport O_2 to the regions of oxidizing of silicon nanocrystals, which are deep in the pores. When the diffusion of oxygen into the pores becomes difficult because of its screening and pushing off by the particles of the nanoporous skeleton, which are ejected from the porous layer, and due to in result of using of O_2 for oxidation of these particles (aerosol regime of combustion), the rate of the propagation of the combustion front slows down with increasing oxygen pressure and in some cases decreases (Fig. 2).

It should be noted that the stoichiometry coefficient of the system "porous layer of a sample – oxygen of the test chamber" lies at pressures of 20–30 bar within $(2–8)\cdot 10^{-4}$ (depending on the Conditions). Thus, even with complete combustion of the porous layer in the case of the aerosol regime, the loss of molecular oxygen does not exceed 0.08%

The imaging process with the aid of DC Fastcam SA-X2 shows that even at P = 20 bar the cloud of burning aerosol and of combustion products has a rather distinct contour and gradually propagates upward. As the initial pressure increases further, the propagation of the aerosol cloud to the region above the sample is enhanced as a rule. The highest increase is observed at high initial pressures, from 27.5 to 32.5 bar. It is caused by both the pressing-out of the central part of the cloud by the expanding gaseous products of combustion and by the gravity forces. The dynamics of the process for one of most intense ejections is shown in Fig. 4, and the graphs of the rise of the formation for specimens of Conditions 7 are presented in Fig. 5. This formation that has a rather distinct shape that transforms with time includes particle of both burning pSi and the products of its combustion.

The possibility of the occurrence of chemical reactions within the formation is indicated by the fast increase of its volume and the high luminosity of the central region, which with time is screened by periphery regions that cool off rapidly as a result of radiation heat transfer.

The importance of the pulse of the gaseous sublayer of combustion products for the effect of the "floating-up" of the object described is confirmed by two facts: the substantial dependence of the rise height on the sample width (in Fig. 5, compare the curves for 10- and 2.3-mm-wide samples in experiments at P = 30 bar) and by the deviation of the floating-up formation from the vertical in the case of asymmetric firing (not at the specimen center). In this case, after the cessation of frontal combustion on the shorter side and the decrease in the pressure of the gaseous sublayer, the floating object starts to deviate toward this side.

An analysis of the results obtained, including the data of Fig. 5, shows that for samples of the same width the height of the rise slowly increases with pressure, however, at pressures 30 and 32.5 bar the behavior of the object core is virtually the same.

The study of the process on asymmetric initiation allows one to draw a conclusion that though the combustion of the aerosol cloud is a highly intense process, but it is not instantaneous and starts with ejection of rather cold particles being heated by radiation from the zone of aerosol combustion and by the heterogeneous oxidation reaction starting on the surface of these particles. An analysis of the curves in Fig. 5 shows that the initial velocity of the rise of aerosol clouds practically does not depend on the parameters of experiment and amounts to about 15 m/s. It should be noted that the velocity of stationary propagation of individual particles at the level of the upper boundary of the aerosol is equal to about 10 m/s, i.e., it is somewhat lower. The angle of ejection of particles from the front of initial combustion

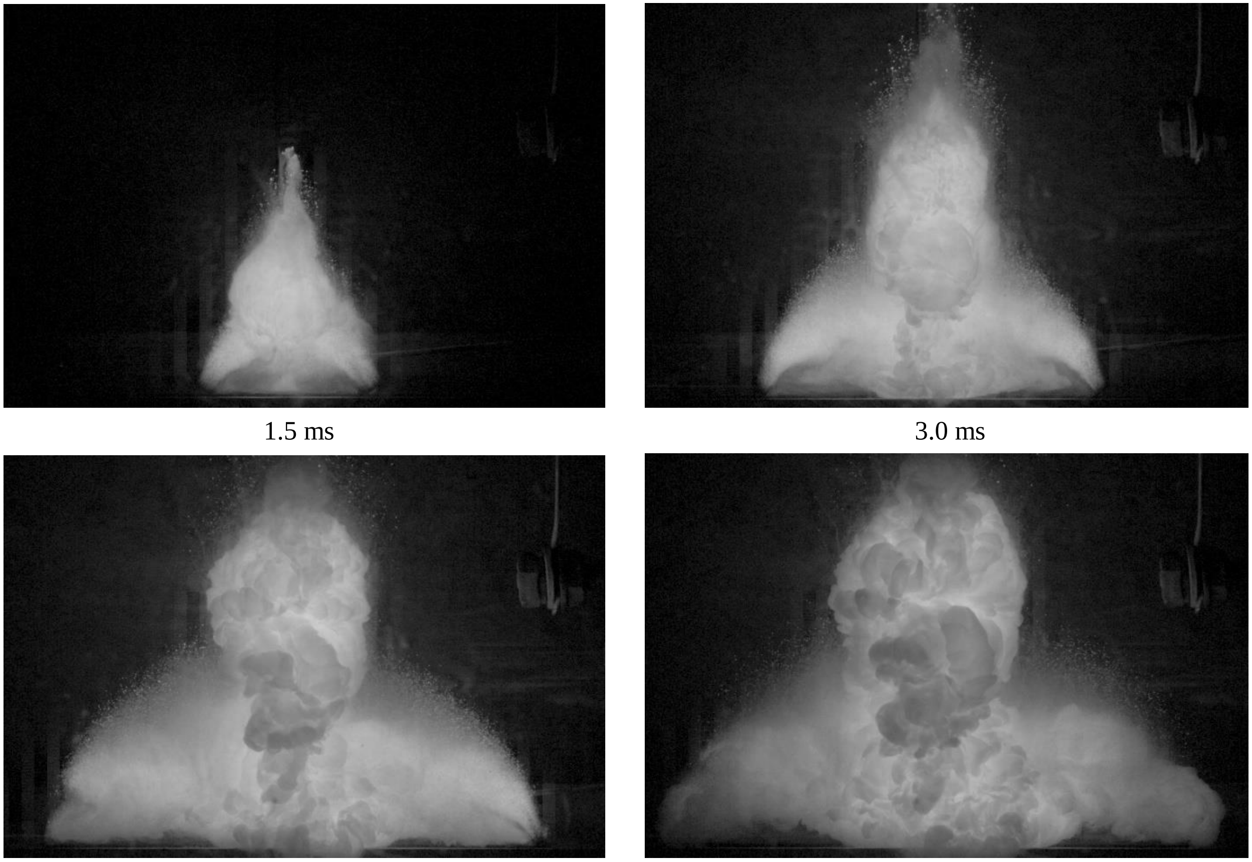

1.5 ms 3.0 ms

4.5 ms 6.0 ms

Figure 4. Dynamics of the process of combustion of pSi sample of width 10 mm at *P* = 30 bar (Conditions 7, figures under the frames indicate time from the instant of ignition).

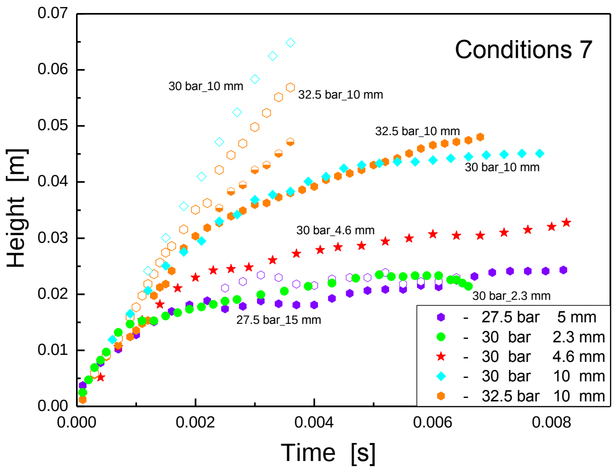

Figure 5. Propagation of the cloud from the particles of burning porous layer and products of its combustion over the height of the working chamber with time; solid symbols, the upper boundary of the object core; light and semi-solid symbols, upper and lower, respectively, boundaries of emission; oxygen pressures and width of samples are indicated in notation.

relative to the sample surface increases with pressure. At some instants of time it exceeds 90°, i.e., particles outrun the front of the surface combustion.

It is interesting that in this region of high pressures, the rate of combustion is virtually independent of the sample width. As a rule, the samples had a width of about 5 mm. At 30 bar, the experiments were carried out with samples whose width is indicated in Fig. 5. The result obtained shows that the edge effects do not exert a substantial influence on the character of combustion, possibly due to the fact that an increase of heat losses near the edge is compensated in this case by the better access of oxidizer into the combustion zone.

The results of the spectral analysis of radiation in the process of combustion of pSi samples within 400–860 nm show that the dynamics of variation of the spectra for samples of different types is similar. As the oxygen pressure increases, the level of short-wave radiation first increases with a possible start of formation of local maxima. Then the maximum of the spectrum begins to move from the near-IR region to the red region and as it moves, the intensity of radiation in the IR region decreases rapidly. As a rule, the transformation of the spectrum, i.e., the increase in the short-wave region radiation contribution and the shift of the maximum toward the saturated red color (720–728 nm), takes place at high oxygen pressures. The temperatures in the zone of combustion, in most cases of the aerosol one, are estimated by the shift of the maximum of recorded radiation spectra. According to the Wien law, in the range of the initial oxygen pressures 20–30 bar, the temperatures lie between 3400 and 4000 K.

On the whole, all recorded spectra are rather smooth and continuous, which is a sufficient condition for the temperature to be measured by the photoemission method [6]. Figure 6 presents the temperature curves for combustion of samples formed in regimes 1 and 2 at different oxygen pressures. It should be noted first of all that the presented fragments of the temperature curves are, as a rule, the first portions where the temperature can be determined with necessary accuracy.

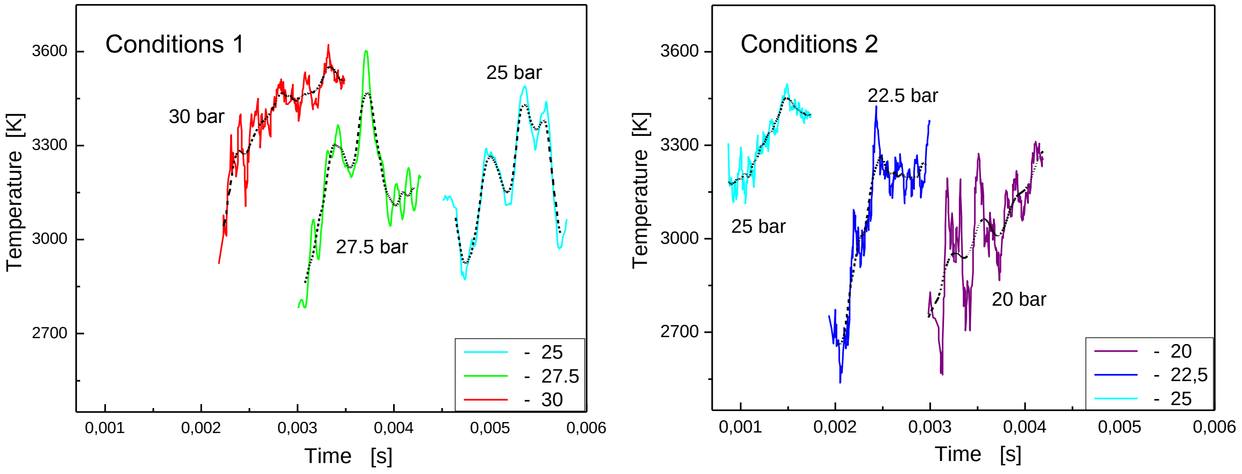

(a) (b)

Figure 6. Temperature curves during combustion of pSi samples at different oxygen pressures (*t* is the time from the instant of spark ignition; in the notation on the graphs, values of pressure in bar, dash line, smooth curves): a) samples formed at Conditions 1; b) samples formed at Conditions 2

This is due to the limitation of the minimum level of the signal acceptable by the program for temperature calculation. Thus, for the used method of temperature measurement, the time before the appearance of the corresponding curve is a certain analog of the time of induction and characterizes the time of "ignition", i.e., formation of a rather powerful combustion zone.

It is seen that in the samples of the same type the "time of induction" decreases with increase in oxygen pressure; in this case, despite the lower level of pressures for samples of Conditions 2, the process of combustion develops more rapidly in them.

An analysis shows that the common tendency is the growth of the process temperatures with increase in the oxygen pressure. For all samples, except for the sample of conditions1 at 25 bar, temperatures of combustion in a gaseous medium are recorded. Since in the case mentioned, the recorded values of temperature correlate well with other results, we may assume that the regime of combustion of porous silicon does not affect the temperature level of the process substantially. The maximum temperatures of the process are attained at oxygen pressures 27.5 and 30 bar and are equal to about 3600 K.

The results obtained show that the processes studied are high-power ones and that porous silicon is a promising material for creating solid fuels on its basis.

Acknowledgment. The work is done within the framework of the State Program of Scientific Research "Energy Systems, Processes, and Technologies", Belarus.

References

[1] Fan GJ, Song XP, Quan MX, Hu ZQ. (1996). Explosive Reaction During the Mechanical Alloying of the Si/PbO System. Scripta Materialia. 35(9): 4.

[2] Mikulec FV, Kirtland JD, Sailor MJ.(2002). Explosive Nanocrystalline Porous Silicon and Its Use in Atomic Emission Spectroscopy. Advanced Materials. 14(1): 38.

[3] Kovalev D, Timoshenko VY, Kunzner N, Gross E, Koch F. (2001). Strong Explosive Interection of Hydrogenated Porous Silicon with Oxygen at Cryogenic Temperatures. Physical Review Letters. 87(6): 068301-1.

[4] Plummer A, Kuznetsov V, Joyner T, Shapter J, Voelcker NH. (2011). The Burning Rate of Energetic Films of Nanostructured Porous Silicon. Small. 7(23): 3392

[5] Grosman A, Ortega C, in Properties of Porous Silicon, edited by L. Canham (INSPEC, London, 1997), p. 145.

[6] Kasparov KN. (2011). Photoemission Analysis of Optical Radiation, Minsk Belaruskaya Nauka Press, 178 p.